

Spin state modulation of iron spin crossover complexes *via* hydrogen-bonding self-assembly†

Cite this: DOI: 10.1039/c3cc42851f

Received 17th April 2013,
Accepted 30th May 2013

DOI: 10.1039/c3cc42851f

www.rsc.org/chemcomm

Iron complexes derived from 6-diaminotriazolyl-2,2'-bipyridines display spin crossover behaviour, and hydrogen bonding-controlled self-assembly with a suitable barbiturate partner can modulate the crossover from mixed low and high spin to high spin. This system is the first to use solution-phase self-assembly of complementary hydrogen-bonding organic species to modulate spin state.

The ability to control molecular states, such as conformation or charge, presents options for creating molecular machines.¹ By controlling molecular motion, nanosized motors,² logic gates,³ and data storage media⁴ have been prepared. Many of these nanoswitches that have been reported currently operate by moving molecules in space.⁵ Nanoswitches can also be designed utilizing transition metal spin crossover (SCO) complexes.⁶ In these complexes, mid-lying ⁵E_g orbitals allow for facile switching between populating ⁵T_{2g} orbitals (low spin) and ⁵E_g orbitals (high spin). First row transition metal complexes, especially those of iron, are widely studied for SCO phenomena.⁷

SCO often occurs in iron complexes when strong-field ligands are modified either sterically or electronically to induce less field-splitting.⁸ SCO is typically regulated thermally, but other perturbations are known, including changes in pressure or photoexcitation.⁹ In iron-containing metal-organic frameworks, SCO has even been linked to structural changes caused by the adsorption and release of certain guests.¹⁰ Even something as simple as binding of an anion can cause mono or polynuclear complexes to undergo spin transition.¹¹ This suggests that an SCO system can be modulated through supramolecular self-assembly of polynuclear metal complexes.

The combination of both metal and hydrogen bonding mediated self-assembly was achieved by using bifunctional ligand **1** (Fig. 1). Ligand **1** has dual functionality in that it contains a tridentate metal chelator, while also displaying a three-point hydrogen bonding diaminotriazine motif.¹² The replacement of a pyridine with a triazine has previously been shown to induce

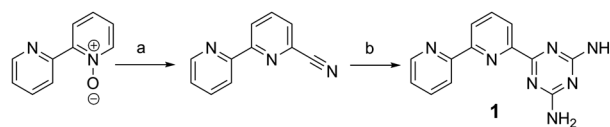


Fig. 1 Synthesis of **1**: (a) PhCOCl, Me₃SiCN, CH₂Cl₂, 5 d, RT (63%); (b) dicyandiamide, KOH, iPrOH, 24 h, 82 °C (71%).

spin crossover in some iron(II)-terpyridine complexes.¹³ Self-assemblies combining *both* metal-coordination and hydrogen bonding are rare, and are typically only observed in the solid state.¹⁴ Synthesis of these species often occurs by growing or precipitating the material as an insoluble network. Achieving hydrogen-bonding self-assembly in polar solvents that can solubilize ionic metal-ligand complexes is far more challenging.

Ligand **1** was synthesized in two steps from the unsymmetrical 2,2'-bipyridine-*N*-oxide (Fig. 1).¹⁵ This was reacted with benzoyl chloride and trimethylsilyl cyanide to give the mononitrile,¹⁶ which was then condensed with dicyandiamide to give **1**.¹⁷ Ligand **1** formed a 2 : 1 adduct with Fe(ClO₄)₂ giving a purple product indicative of a low spin Fe(II) bis-terpyridine complex.

The ¹H-NMR of (1)₂·Fe·(ClO₄)₂ showed a significant amount of paramagnetic character at room temperature, with proton resonances ranging from above 25 to below 0 ppm, suggesting that both high spin and low spin states were present. Solution-phase magnetic susceptibility measurements in DMSO showed a μ_{eff} of 4.4, consistent with a mix of spin states between 0 (low spin) and 2 (high spin). While ligand **1** did not display significant solubility in solvents other than DMSO, (1)₂·Fe·(ClO₄)₂ was remarkably soluble in a variety of organic solvents.

An X-ray quality crystal of this complex was grown by diffusion of benzene into an acetonitrile solution of (1)₂·Fe·(ClO₄)₂ (Fig. 2). The structure shows that the iron is in a distorted octahedral environment. The bond angle between the outer pyridine and triazine nitrogen atoms is approximately 161°. The bond distances range from ~1.89 Å for the inner pyridine Fe–N, to ~2.05 Å for the triazine Fe–N. These bond distances are consistent with a low spin octahedral Fe(II) complex.¹⁸ This suggests that the iron is mostly if not completely low spin at 100° K. There is also evidence from the solid state structure that a small amount of hydrogen bonding

Department of Chemistry, University of California - Riverside, 501 Big Springs Rd., Riverside, CA, 92521, USA. E-mail: richard.hooley@ucr.edu

† Electronic supplementary information (ESI) available: Synthesis and characterization of new compounds. CCDC 934197. For ESI and crystallographic data in CIF or other electronic format see DOI: 10.1039/c3cc42851f

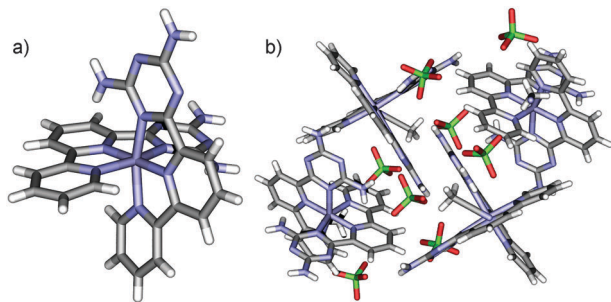


Fig. 2 Crystal Structure of $(1)_2\cdot\text{Fe}\cdot(\text{ClO}_4)_2$: (a) view of a single $(1)_2\cdot\text{Fe}$ unit; (b) a view of the unit cell of $(1)_2\cdot\text{Fe}\cdot(\text{ClO}_4)_2$ showing the twisting of the triazine units as well as the weak hydrogen bonding to the perchlorate counterions.

occurs between the triazine protons and the perchlorate counterions. When $(1)_2\cdot\text{Fe}\cdot(\text{BF}_4)_2$ and $(1)_2\cdot\text{Fe}\cdot(\text{BPh}_4)_2$ were prepared for comparison, they gave NMR spectra similar to $(1)_2\cdot\text{Fe}\cdot(\text{ClO}_4)_2$, showing the paramagnetic effect is not significantly affected by removal of hydrogen bonding with the counterion.

UV/Vis spectroscopy of $(1)_2\cdot\text{Fe}\cdot(\text{ClO}_4)_2$ showed a metal–ligand charge-transfer band at 557 nm, similar to that of known low spin octahedral Fe(II)-terpyridine complexes.¹⁹ Variable temperature UV/Vis spectroscopy showed the intensity of this band to be inversely proportional to temperature, further consistent with SCO (see ESI[†]). This transition could also be followed by variable temperature NMR. Lowering the temperature caused a decrease in chemical shift (Fig. 3),²⁰ and magnetic susceptibility measurements assessed by the Evans' method confirmed that the μ_{eff} of the complex also decreased (see ESI[†]).

The core complex $(1)_2\cdot\text{Fe}\cdot(\text{ClO}_4)_2$ can be assembled into larger solution-phase aggregates by combining the iron(II)-diaminotriazine species with an organic soluble dialkylbarbiturate. This motif is known to favor self-assembly in a number of hydrogen-bonded multi-component assemblies.²¹ When dioctyl barbiturate **2**²² was combined with $(1)_2\cdot\text{Fe}\cdot(\text{ClO}_4)_2$ in either MeCN-*d*₃ or Me₂CO-*d*₆, the bipyridyl resonances of $(1)_2\cdot\text{Fe}\cdot(\text{ClO}_4)_2$ shifted slightly downfield in the ¹H-NMR spectrum, corresponding to a fast exchange between unbound and self-assembled species (Fig. 4). Addition of **2** to $(1)_2\cdot\text{Fe}\cdot(\text{ClO}_4)_2$ also gave rise to a new set of peaks which appeared to be diamagnetic and were in slow exchange with the other species in solution. As the concentration of **2** was increased relative to $(1)_2\cdot\text{Fe}\cdot(\text{ClO}_4)_2$, the

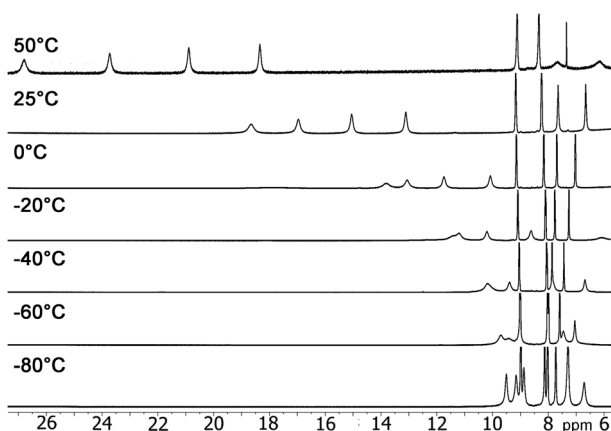


Fig. 3 ¹H-NMR spectra of $(1)_2\cdot\text{Fe}\cdot(\text{ClO}_4)_2$ at varying temperatures (acetone-*d*₆, 500 MHz).

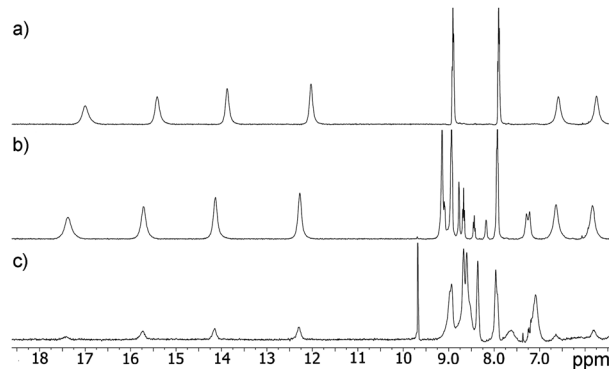


Fig. 4 ¹H-NMR spectra of (a) $(1)_2\cdot\text{Fe}\cdot(\text{ClO}_4)_2$; (b) the mixture of species observed upon addition of **2** (0.66 equiv.) to $(1)_2\cdot\text{Fe}\cdot(\text{ClO}_4)_2$; (c) saturation of **2** added to $(1)_2\cdot\text{Fe}\cdot(\text{ClO}_4)_2$ (CD₃CN, 400 MHz, 1.4×10^{-2} M, 298 K).

“diamagnetic” species predominated. Changing the counter ion to BF₄ had no effect on the NMR spectra nor did reversing the order of addition. The end point for the titration could not be determined by NMR due to the limited solubility of **2** in acetonitrile.

Analysis of the titration of **2** into a solution of $(1)_2\cdot\text{Fe}\cdot(\text{ClO}_4)_2$ by UV/Vis spectroscopy showed clear *reduction* of the MLCT band at 557 nm with increasing concentration of **2** (Fig. 5). The band was replaced by a growing shoulder at 370 nm corresponding to the MLCT of a high spin iron(II) complex. This data suggests (in conflict with the more upfield-shifted ¹H-NMR) that upon self-assembly with dioctylbarbiturate **2**, a magnetically silent motif, spin transition occurs in the central iron atom: $(1)_2\cdot\text{Fe}\cdot(\text{ClO}_4)_2$ is switched from a mixed low/high to a high spin state simply by hydrogen-bonding self-assembly. Cyclic voltammetry analysis of the $(1)_2\cdot\text{Fe}\cdot\mathbf{2}$ assembly corroborated this observation. The free complex $(1)_2\cdot\text{Fe}\cdot(\text{BPh}_4)_2$ gave one oxidation and reduction potential (see ESI[†]; the BPh₄ salt was used as a redox-inactive counterion). Upon addition of **2**, multiple oxidations were observed, consistent with iron in different environments present in solution. After saturation with barbiturate only a single, lower oxidation potential was observed, consistent with all of the iron now being in a new structure.

Attempts to characterize a discrete supramolecular hydrogen-bonded aggregate were unsuccessful. The binding affinity of diaminotriazines for barbiturates is not large in polar solvents, and the complex $[(1)_2\cdot\text{Fe}]^{2+}$ is poorly soluble in non-polar solvents that aid hydrogen-bonding self-assembly. X-ray quality single crystals of a single self-assembled species could not be obtained, even when

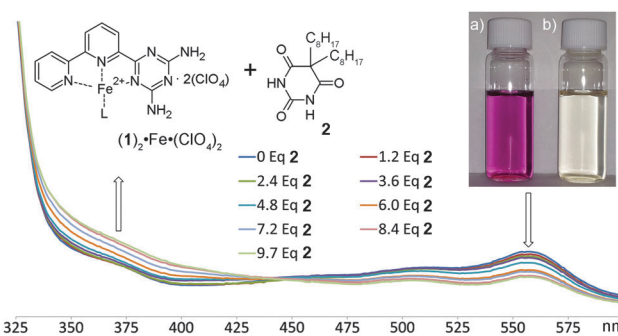


Fig. 5 UV/Vis spectra showing decrease in the low spin MLCT band and increase in the high spin MLCT band as **2** is added to $(1)_2\cdot\text{Fe}\cdot(\text{ClO}_4)_2$ (2.6×10^{-6} M, MeCN). Inset: (a) $(1)_2\cdot\text{Fe}\cdot(\text{ClO}_4)_2$ alone; (b) +20 equiv. **2**.

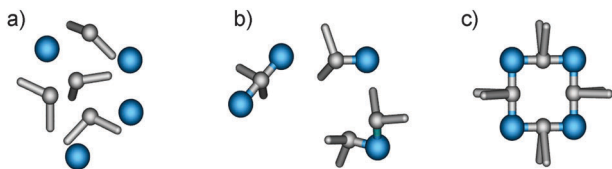


Fig. 6 Cartoon showing the possible assemblies of $[(1)_2\text{-Fe}(\text{ClO}_4)_2]_x \cdot 2_y$: (a) free $(1)_2\text{-Fe}(\text{ClO}_4)_2$ and **2**; (b) partially assembled $[(1)_2\text{-Fe}(\text{ClO}_4)_2]_x \cdot 2_y$; (c) closed $[(1)_2\text{-Fe}(\text{ClO}_4)_2]_4 \cdot 2_4$.

using the tetraphenyl borate salt. Diffusion NMR was investigated as a possible analysis tool, but the exchange between aggregates occurred rapidly on the diffusion timescale, and all of the diffusion coefficients were on the expected order for small molecules.

Molecular modelling analysis suggested that a plausible identity for this assembly was a square: $[(1)_2\text{-Fe}(\text{ClO}_4)_2]_4 \cdot 2_4$ (see ESI† for structure). Fig. 6 shows a cartoon representation of the assembly process. Addition of **2** to the $(1)_2\text{-Fe}(\text{ClO}_4)_2$ complex leads to undefined aggregates (Fig. 6b) which ultimately leads to a more stable “closed” assembly (Fig. 6c). These components exchange rapidly on the NMR timescale in solution, and the assemblies are observed as an averaged signal of all the equilibrating aggregates until reaching the more stable species.

To show that the complete spin transition is due to the self-assembly of multiple iron-containing complexes, 3,3-dimethylglutarimide **3** was added to the system (see ESI† for spectra). **3** provides similar hydrogen-bonding properties as **2**, but cannot form aggregates containing multiple Fe ions, rather a single 2 : 1 complex with $(1)_2\text{-Fe}(\text{ClO}_4)_2$. Upon addition of **3** to a solution of $(1)_2\text{-Fe}(\text{ClO}_4)_2$, no diamagnetic aggregates were observed by $^1\text{H-NMR}$, even with a 600-fold excess of **3**. UV/Vis analysis of the titration of **3** into $(1)_2\text{-Fe}(\text{ClO}_4)_2$ showed no change in absorbance spectrum upon addition of excess **3**, indicating that the variance in spin crossover behaviour is truly a supramolecular effect, caused by the hydrogen bond-mediated self-assembly of multiple iron-containing species.

Similar SCO behaviour was also observed for the Fe(III) analog. $(1)_2\text{-Fe}(\text{ClO}_4)_3$ was prepared in a similar manner from **1** and $\text{Fe}(\text{ClO}_4)_3 \cdot x\text{H}_2\text{O}$, giving an orange complex. The $^1\text{H-NMR}$ spectrum for this paramagnetic species was much sharper, and all of the peaks fell within a standard 14 to -2 ppm range on the spectrometer (see ESI†). Magnetic susceptibility measurements and VT-NMR showed that $(1)_2\text{-Fe}(\text{ClO}_4)_3$ also displayed SCO behaviour. The μ_{eff} of 3.5 at room temperature showed the iron was mixed between $S = \frac{1}{2}$ for low spin Fe(III) and $S = 2\frac{1}{2}$ for high spin. When $(1)_2\text{-Fe}(\text{ClO}_4)_3$ was combined with **2**, the NMR peaks began to shift, although no new species appeared as **2** was added. UV/Vis showed a similar trend however, as the MLCT band observed at 380 nm disappeared as barbiturate was added.

The exact cause of spin modulation upon hydrogen bonding mediated self-assembly of $(1)_2\text{-Fe}(\text{ClO}_4)_x$ is not completely evident. It is possibly caused by lengthening of the Fe–N bonds to alleviate strain upon forming the thermodynamically favored closed structure of the assembly.⁸ If the Fe–N bonds are stretched far enough, it follows that the relative shifts of the proton resonances will decrease.²³ Alternatively, the diamagnetic characteristics of the NMR could be the result of antiferromagnetic coupling of the high spin Fe(II). While examples of SCO-modulation are common in solid state and solution-phase bimetallic complexes, the exploitation of

this effect through hydrogen-bonded self-assembly is a novel method of controlling spin states in solution-phase systems. This can serve as a starting point to study these systems as potential solution-phase magnetic switches, and further studies on the supramolecular properties of spin crossover systems are underway in our laboratory.

The authors are grateful to the NSF (CHE-1151773 for R.J.H. and DGE-0813967 for J.A.) and the University of California, Riverside (Dissertation Research Grant for M.C.Y.) for support of this work. Dr Dan Borchardt and Mr Yi Meng are acknowledged for assistance with NMR, Dr Fook Tham for collecting X-Ray diffraction data, and Prof. Vincent Lavallo and Prof. David Bocian for stimulating discussions.

Notes and reference

- 1 J. Wang and B. L. Feringa, *Science*, 2011, **331**, 1429.
- 2 S. P. Fletcher, F. Dumur, M. M. Pollard and B. L. Feringa, *Science*, 2005, **310**, 80.
- 3 (a) D. Margulies, G. Melman and A. Shanzer, *J. Am. Chem. Soc.*, 2006, **128**, 4865; (b) Y. Liu, A. Offenhäuser and D. Mayer, *Angew. Chem., Int. Ed.*, 2010, **49**, 2595.
- 4 J. Wang, L. Hou, W. R. Browne and B. L. Feringa, *J. Am. Chem. Soc.*, 2011, **133**, 8162.
- 5 (a) P. L. Anelli, N. Spencer and J. F. Stoddart, *J. Am. Chem. Soc.*, 1991, **113**, 5131; (b) S. M. Landge and I. Aprahamian, *J. Am. Chem. Soc.*, 2009, **131**, 18269; (c) V. A. Azov, A. Schlegel and F. Diederich, *Angew. Chem., Int. Ed.*, 2005, **44**, 4635.
- 6 C. W. Machan, M. Adelhardt, A. A. Sarjeant, C. L. Stern, J. Sutter, K. Meyer and C. A. Mirkin, *J. Am. Chem. Soc.*, 2012, **134**, 16921.
- 7 A. Bousseksou, G. Molnár, L. Salmon and W. Nicolazzi, *Chem. Soc. Rev.*, 2011, **40**, 3313.
- 8 J. Olguin and S. Brooker, *Coord. Chem. Rev.*, 2011, **255**, 203.
- 9 (a) J. J. Scepaniak, T. D. Harris, C. S. Vogel, J. Sutter, K. Meyer and J. M. Smith, *J. Am. Chem. Soc.*, 2011, **133**, 3824; (b) P. Gütllich, V. Ksenofontov and A. B. Gaspar, *Coord. Chem. Rev.*, 2005, **249**, 1811.
- 10 (a) P. D. Southon, L. Liu, E. A. Fellows, D. J. Price, G. J. Halder, K. W. Chapman, B. Moubaraki, K. S. Murray, J.-F. Letard and C. J. Kepert, *J. Am. Chem. Soc.*, 2009, **131**, 10998; (b) G. J. Halder, C. J. Kepert, B. Moubaraki, K. S. Murray and J. D. Cashion, *Science*, 2002, **298**, 1762.
- 11 (a) C. M. Klug, A. M. McDaniel, S. R. Fiedler, K. A. Schulte, B. S. Newell and M. P. Shores, *Dalton Trans.*, 2012, **41**, 12577; (b) Z. Ni, A. M. McDaniel and M. P. Shores, *Chem. Sci.*, 2010, **1**, 615; (c) R. A. Bilbeisi, S. Zarra, H. L. C. Feltham, G. N. L. Jameson, J. K. Clegg, S. Brooker and J. R. Nitschke, *Chem.-Eur. J.*, 2013, DOI: 10.1002/chem.201300805.
- 12 (a) J. P. Mathias, E. E. Simanek, J. A. Zerkowski, C. T. Seto and G. M. J. Whitesides, *J. Am. Chem. Soc.*, 1994, **116**, 4316; (b) Q. Huo, K. C. Russell and R. M. Leblanc, *Langmuir*, 1998, **14**, 2174.
- 13 S. K. Hain, F. W. Heinemann, K. Gieb, P. Müller, G. Hörner and A. Grohmann, *Eur. J. Inorg. Chem.*, 2010, 221.
- 14 (a) J.-J. Jang, L. Li, T. Yang, D.-B. Kuang, W. Wang and C.-Y. Su, *Chem. Commun.*, 2009, 2387; (b) C.-L. Chen and A. M. Beatty, *J. Am. Chem. Soc.*, 2008, **130**, 17222.
- 15 F. W. J. Demnitz and M. B. D'heni, *Org. Prep. Proced. Int.*, 1998, **30**, 467.
- 16 J. I. Van der Vlug, S. Demeshko, S. Dechert and F. Meyer, *Inorg. Chem.*, 2008, **47**, 1576.
- 17 (a) F. H. Case, *J. Org. Chem.*, 1966, **31**, 2398; (b) A. Duong, T. Maris, O. Lebel and J. D. Wuest, *J. Org. Chem.*, 2011, **76**, 1333.
- 18 E. A. Medlycott, G. S. Hanan, T. S. M. Abedin and L. K. Thompson, *Polyhedron*, 2008, **27**, 493.
- 19 E. C. Constable, G. Baum, E. Bill, R. Dyson, R. van Eldik, D. Fenske, S. Kaderli, D. Morris, A. Neubrand, M. Neuburger, D. R. Smith, K. Wieghardt, M. Zehnder and A. D. Zuberbühler, *Chem.-Eur. J.*, 1999, **5**, 498.
- 20 (a) E. Breunin, M. Ruben, J.-M. Lehn, F. Renz, Y. Garcia, V. Ksenofontov, P. Gütllich, E.-W. Gelgius and K. Rissanen, *Angew. Chem., Int. Ed.*, 2000, **39**, 2504; (b) E. R. King, G. T. Sazama and T. A. Betley, *J. Am. Chem. Soc.*, 2012, **134**, 17858.
- 21 D. C. Sherrington and K. A. Taskinen, *Chem. Soc. Rev.*, 2001, **30**, 83.
- 22 S. M. S. Chauhan and N. G. Giri, *Supramol. Chem.*, 2008, **20**, 743.
- 23 O. A. Gansow, M. R. Willcott and R. E. Lenkinski, *J. Am. Chem. Soc.*, 1971, **93**, 4295.